Effect of substitution of lutetium by gadolinium on emission characteristics of $(Lu_xGd_{1-x})_2SiO_5$: Sm^{3+} single crystals

W. Ryba-Romanowski,[1] A. Strzęp,[1,*] R. Lisiecki,[1] M. Berkowski,[2] H. Rodriguez-Rodriguez[3] and I.R. Martin[3,4]

[1]*Institute of Low Temperature and Structure Research, Polish Academy of Sciences, Wroclaw, Poland,*
[2]*Institute of Physics, Polish Academy of Sciences, Warsaw, 20036, Poland*
[3]*Dep. Fisica Fundamental y Experimental, Electronica y Sistemas, Universidad de la Laguna, La Laguna, Tenerife, Spain*
[4]*MALTA Consolider Team, Instituto de Materiales y Nanotechnologia (IMN), Universidad de la Laguna, La Laguna, Tenerife, Spain*
[*]*a.strzep@int.pan.wroc.pl*

Abstract: Single crystals of $(Lu_xGd_{1-x})_2SiO_5$:Sm (0.5 at%) with x = 0.19 (81% Gd^{3+}) and x = 0.11 (89% Gd^{3+}) belonging respectively to the C2/c and $P2_1/c$ space groups were grown by the Czochralski method under nitrogen atmosphere. Detailed investigation of their spectroscopic properties were performed with the aim of understanding the effect of structural modification on emission characteristics of incorporated Sm^{3+} ions with a special attention directed to a laser potential associated with yellow emission line. It was inferred from low temperature optical spectra that almost all emission intensity in the host with C2/c symmetry comes from one of two available Sm^{3+} sites, whereas two Sm^{3+} sites contribute to emission in the host with $P2_1/c$ symmetry. Excitation spectra of Sm^{3+} emission recorded in the VUV-UV region between 100 nm and 350 nm made it possible to locate the energy of CT transition at about 6.11 eV and to assess the low energy limit for the $4f^5 \rightarrow 4f^4 5d^1$ transitions of Sm^{3+} to about 6.81 eV. It implies that in the two systems studied these energies are advantageously high thereby preventing the contribution of intense allowed transitions to an adverse excited state absorption of both blue pump radiation and yellow emission. Experiments of optical amplification of yellow emission were performed employing a pump-and-probe technique in order to verify this implication. It was found that for a LGSO:Sm^{3+} crystal having the C2/c symmetry an increase of the pump power density from 20 mJ/cm^2 to 50 mJ/cm^2 at a constant power probe density of 150 μW/cm^2 brings about a positive gain growing from about 0.25 to 2 [cm^{-1}]. In the same conditions a maximum gain value of 1 cm^{-1} was measured for LGSO:Sm^{3+} crystal having the $P2_1/c$ symmetry. It was concluded that the former system is promising for the design of all-solid-state yellow lasers.

OCIS codes: (140.3380) Laser materials; (140.3480) Lasers, diode-pumped; (140.5680) Rare earth and transition metal solid-state lasers.

References and links

1. H. Suzuki, T. A. Tombrello, C. L. Melcher, and J. S. Schweitzer, "UV and gamma-ray excited luminescence of cerium-doped rare earth oxyorthosilicates," Nucl. Instrum. Methods Phys. Res. **320**(1-2), 263–272 (1992).
2. C. L. Melcher and J. S. Schweitzer, "A promising new scintillator: cerium-doped lutetium oxyorthosilicate," Nucl. Instrum. Methods Phys. Res. A **314**(1), 212–214 (1992).
3. N. V. Kuleshov, V. G. Shcherbitsky, A. A. Lagatsky, V. P. Mikhailov, B. I. Minkov, T. Danger, T. Sandrock, and G. Huber, "Spectroscopy, excited-state absorption and stimulated emission in Pr^{3+}-doped Gd_2SiO_5 and Y_2SiO_5 crystals," J. Lumin. **71**(1), 27–35 (1997).

#205162 - $15.00 USD Received 21 Jan 2014; revised 6 Mar 2014; accepted 6 Mar 2014; published 18 Mar 2014

4. G. Dominiak-Dzik, W. Ryba-Romanowski, R. Lisiecki, P. Solarz, and M. Berkowski, "Dy-doped Lu_2SiO_5 single crystal: spectroscopic characteristics and luminescence dynamics," Appl. Phys. B **99**(1-2), 285–297 (2010).
5. R. Lisiecki, G. Dominiak-Dzik, P. Solarz, W. Ryba-Romanowski, M. Berkowski, and M. Głowacki, "Optical spectra and luminescence dynamics of the Dy-doped Gd_2SiO_5 single crystal," Appl. Phys. B **98**(2-3), 337–346 (2010).
6. A. S. S. de Camargo, M. R. Davolos, and L. A. O. Nunes, "Spectroscopic characteristics of Er^{3+} in the two crystallographic sites of Gd_2SiO_5," J. Phys. Condens. Matter **14**(12), 3353–3363 (2002).
7. Y. Chen, B. Liu, Ch. Shi, M. Kirm, M. True, S. Vielhauer, and G. Zimmerer, "Luminescent properties of Gd_2SiO_5 powder doped with Eu^{3+} under VUV–UV excitation," J. Phys. Condens. Matter **17**(7), 1217–1224 (2005).
8. A. Strzęp, R. Lisiecki, P. Solarz, G. Dominiak-Dzik, W. Ryba-Romanowski, and M. Berkowski, "Optical spectra and excited state relaxation dynamics of Sm^{3+} in Gd_2SiO_5 single crystal," Appl. Phys. B **106**(1), 85–93 (2012).
9. C. Li, R. Moncorge, J. C. Souriau, C. Borel, and Ch. Wyon, "Efficient 2.05 μm room temperature Y_2SiO_5:Tm^{3+} cw laser," Opt. Commun. **101**(5-6), 356–360 (1993).
10. C. Yan, G. Zhao, L. Su, X. Xu, L. Hang, and J. Xu, "„Growth and spectroscopic characteristics of Yb:GSO single crystal," J. Phys. Condens. Matter **18**(4), 1325–1333 (2006).
11. M. Jacquemet, C. Jacquemet, N. Janel, F. Druon, F. Balembois, P. Georges, J. Petit, B. Viana, D. Vivien, and B. Ferrand, "Efficient laser action of Yb:LSO and Yb:YSO oxyorthosilicates crystals under high-power diode-pumping," Appl. Phys. B **80**(2), 171–176 (2005).
12. G. B. Loutts, A. I. Zagumennyi, S. V. Lavrishchev, Yu. D. Zavartsev, and P. A. Studenikin, "„Czochralski growth and characterization of $(Lu_{1-x}Gd_x)_2SiO_5$ single crystals for scintillators," J. Cryst. Growth **174**(1-4), 331–336 (1997).
13. O. Sidletskiy, V. G. Bondar, B. V. Grynyov, D. A. Kurtsev, V. N. Baumer, K. N. Belikov, Z. V. Shtitelman, S. A. Tkachenko, O. V. Zelenskaya, N. G. Starzhinsky, and V. A. Tarasov, "Growth of LGSO: Ce crystals by the Czochralski method," Crystallogr. Rep. **54**(7), 1256–1260 (2009).
14. O. Sidletskiy, V. Bondar, B. Grinyov, D. Kurtsev, V. Baumer, K. Belikov, K. Katrunov, N. Starzhinsky, O. Tarasenko, V. Tarasov, and O. Zelenskaya, "Impact of Lu/Gd ratio and activator concentration on structure and scintillation properties of LGSO:Ce crystals," J. Cryst. Growth **312**(4), 601–606 (2010).
15. M. Głowacki, G. Dominiak-Dzik, W. Ryba-Romanowski, R. Lisiecki, A. Strzęp, T. Runka, M. Drozdowski, V. Domukhovski, R. Diduszko, and M. Berkowski, "Growth conditions, structure, Raman characterization and optical properties of Sm-doped $(Lu_xGd_{1-x})_2SiO_5$ single crystals grown by the Czochralski method," J. Solid State Chem. **186**, 268–277 (2012).
16. P. Haro-Gonzales, I. R. Martin, F. Lahoz, S. Gonzales-Perez, E. Cavalli, and N. E. Capuj, "Optical amplification in Er^{3+}-doped transparent $Ba_2NaNb_5O_{15}$ single crystal at 850 nm," J. Appl. Phys. **106**(11), 113108 (2009).
17. J. Felsche, "The crystal chemistry of the rare-earth silicates," Structure and Bonding **13**, 99–197 (1973).
18. L. Pidol, B. Viana, A. Galtayries, and P. Dorenbos, "Energy levels of lanthanide ions in a $Lu_2Si_2O_7$ host," Phys. Rev. B **72**(12), 125110 (2005).
19. P. Dorenbos, T. Shalapska, G. Stryganyuk, A. Gektin, and A. Voloshinovskii, "Spectroscopy and energy level location of the trivalent lanthanides in $LiYP_4O_{12}$," J. Lumin. **131**(4), 633–639 (2011).
20. P. Dorenbos, "Systematic behaviour in trivalent lanthanide charge transfer energies," J. Phys. Condens. Matter **15**(49), 8417–8434 (2003).
21. K. Mori, M. Nakayama, and H. Nishimura, "Role of the core excitons formed by 4f-4f transitions of Gd^{3+} on Ce^{3+} scintillation in Gd_2SiO_5," Phys. Rev. B **67**(16), 165206 (2003).
22. D. Navarro-Urrios, M. Melchiorri, N. Daldosso, L. Pavesi, C. García, P. Pellegrino, B. Garrido, G. Pucker, F. Gourbilleau, and R. Rizk, "Optical losses and gain in silicon-rich silica waveguides containing Er ions," J. Lumin. **121**(2), 249–255 (2006).

1. Introduction

The rare earth oxyorthosilicate compounds Re_2SiO_5 (Re^{3+} = Y, Gd, Lu) form hard, transparent, optically biaxial crystals. They melt congruently thereby large single crystals can be grown by the Czochralski method. These features, combined with an ability to incorporate appreciable quantities of luminescent rare earth ions have pointed at a potential of these hosts for a design of practically useful luminescent materials. In fact, crystals Gd_2SiO_5 (GSO), Y_2SiO_5 (YSO) and Lu_2SiO_5 (LSO) doped with Ce^{3+} ions have been intensively studied in the past owing to their promising scintillation properties [1]. Among them the Lu_2SiO_5:Ce scintillating crystal was found to be of particular interest because of its high light output (27300 photons/MeV), suitable emission wavelength (420 nm) and short decay time (~40 ns) [2]. Later on, numerous papers were devoted to spectroscopic investigation of oxyorthosilicate crystals doped with various rare earth ions, e.g. Pr^{3+} [3], Dy^{3+} [4,5], Eu^{3+} [6,7], Sm^{3+} [8], or Tm^{3+} [9]. When doped with ytterbium ions the LSO crystal proved to be a promising laser material emitting in near infrared [10, 11]. Unfortunately, a melting point above 2000 °C and a very high price of lutetium oxide Lu_2O_3 put the Lu_2SiO_5 host at a disadvantage of manufacturing process. On the other hand, GSO crystals show strong

#205162 - $15.00 USD Received 21 Jan 2014; revised 6 Mar 2014; accepted 6 Mar 2014; published 18 Mar 2014

tendency to cleave thus posing serious problems during mechanical processing. Solid solution crystals $(Lu_xGd_{1-x})_2SiO_5$ (LGSO) have been considered aiming to overcome these drawbacks. Investigation on growth, crystal structure and scintillation characteristics of cerium-doped LGSO host has revealed that LGSO forms crystals belonging to the C2/c space group inherent to LSO for x value above 0.2 and to the $P2_1/c$ space group inherent to GSO for x value below 0.2 [12–14]. In a more recent paper it has been reported that the change of the LGSO symmetry occurs at $0.15 < x < 0.17$ [15]. It has been ascertained also that the melting point of LGSO diminishes monotonously with decreasing Lu/Gd ratio and becomes inferiour to 1800 °C when $x \leq 0.2$ [15]. Thus, the choice of the LGSO host for luminescent rare earth ions allows to drop advantageously both the crystallization temperature and the cost of chemicals, thereby making practical applications of these systems more favourable.

Interest in LGSO:Sm^{3+} crystals considered in the present work stems from the fact that they have an ability to convert an UV- blue emission of InGaN/GaN laser diodes into efficient visible emission distributed into green, yellow and red bands. In our opinion the spectral distribution of this emission reported in [15] is promising for application purposes, namely in the design of quasi-white light sources and possibly all-solid-state yellow laser. Systematic examination of structural peculiarities and of room temperature optical spectra of $(Lu_xGd_{1-x})_2SiO_5:Sm^{3+}$ single crystals with $0.11 < x < 0.50$ has revealed that spectroscopic features of Sm^{3+} change markedly when the change of Lu/Gd ratio induces the structural transition of the host [15]. Intentions of the present work are: *(i)* to understand the effect of structural modification mentioned above and *(ii)* to get a more detailed knowledge on the emission ability of materials studied. For these purposes low temperature emission spectra in the visible and excitation spectra in the VUV region and VUV-excited emission spectra were recorded and examined. Spectral features in the VUV region were investigated aiming at assessment of susceptibility of the systems under study to parasitic excited state absorption (ESA), an adverse phenomenon able to affect strongly the emission in Pr^{3+}-doped Gd_2SiO_5 and Y_2SiO_5 crystals [3]. In the last section of the work results of experiments devoted to the evaluation of optical amplification of yellow emission in LGSO:Sm^{3+} crystals are presented.

2. Experimental

Single crystals of $(Lu_xGd_{1-x})_2SiO_5$:Sm (0.5 at%) with x = 0.19 (81%Gd^{3+}) and x = 0.11 (89%Gd^{3+}) belonging respectively to the C2/c and $P2_1/c$ space groups were grown by the Czochralski method under nitrogen atmosphere. The manufacturing details have been reported elsewhere [15]. Transparent and colourless crystals with 20 mm of the diameter were grown from the 40 mm crucible. The plates with the (100) orientation were cut from crystal boules, polished and used in experiment. A strong tendency to crack parallel to the cleavage plane (100) was observed for samples cut from crystals with x = 0.11

Absorption spectra were recorded employing a Varian 5E UV-VIS-NIR spectrophotometer with a spectral bandwidth set to 0.5 nm. Measurement of luminescence spectra was carried out using an Optron Dong-Woo Fluorometer System containing an ozone-free Xe lamp as an excitation source. In this experiment an incident light at wavelength λ_{exc} = 405 nm was chosen by means of an excitation monochromator to match an intense absorption line of Sm^{3+} ions. When recording luminescence decay curves a Surelite Optical Parametric Oscillator (OPO) pumped by a third harmonic of a Nd:YAG laser was used as an excitation source. The emitted light was dispersed by a grating monochromator and detected by a photomultiplier connected to a Tektronix TDS 3052 oscilloscope. To record spectra and decay curves as a function of temperature a continuous flow liquid helium cryostat working in the 4 K – 300 K range was employed.

Measurement of excitation spectra in a vacuum-ultraviolet (VUV) region and VUV-excited emission spectra was carried out using a set-up available at the SUPERLUMI station of Synchrotronstrahlungslabor (HASYLAB) at Deutsche Elektronen-Synchrotron (DESY) in Hamburg. Samples were mounted on a finger of a helium cryostat and measured at 12 K and 300 K. Excitation spectra were corrected for the incident flux of the excitation beam using the

#205162 - $15.00 USD Received 21 Jan 2014; revised 6 Mar 2014; accepted 6 Mar 2014; published 18 Mar 2014

sodium salicylate as a standard. Emission spectra under the VUV excitation (λ_{exc} = 50 – 333 nm) were recorded with a CCD camera.

The optical amplification experiments were carried out in a pump and probe experimental setup, shown in [16]. The pump radiation was provided by an optical parametric oscillator (OPO) (EKSPLA, NT 342/3/UVE) tuned at 473 nm with high energy pulses between 0.01 and 0.05 [J/cm^2] with duration of 10 ns. The monochromatic probe beam was obtained by dispersing the light of Oriel Xenon 400 W lamp with a monochromator Oriel 7725 1/8m, giving a signal power density of 150 μW/cm^2 at 600 nm with a spectral FWHM of 4 nm. The studied samples were placed after a 1 mm diameter pinhole. The incidence of pump and probe beams were parallel and normal to the surface of the samples, which ones were cut and polished in order to have good optical faces with a similar thickness of 0.36 cm. In order to cover the whole area of the pinhole, the pump and probe were focused on pinhole area. The detection system was made with a TRIAX-180 monochromator and registered by a digital oscilloscope TEKTRONIX-2430A.

3. Results and discussion

3.1. Room temperature absorption and emission spectra

When interpreting experimental results we will refer to energy level diagram of Sm^{3+} depicted in Fig. 1. It consists of two groups of excited levels separated by relatively large energy gap of

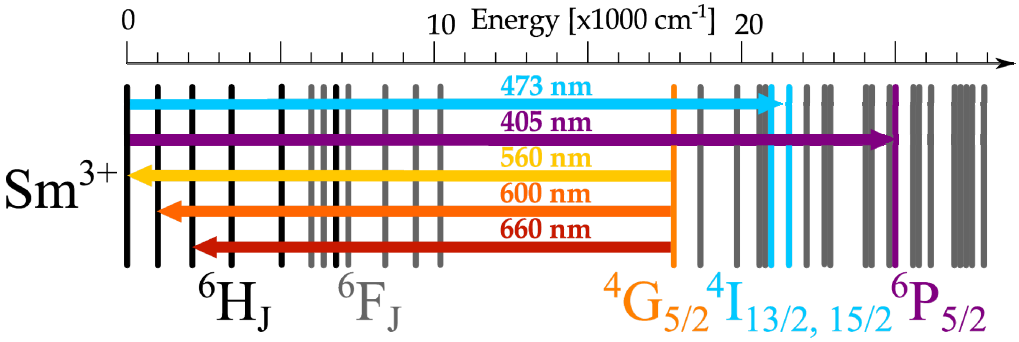

Fig. 1. Energy level diagram for Sm^{3+} ions. Right arrows indicate excitation wavelengths in VIS region, while left arrows emission transitions observed.

about 7000 cm^{-1}. In the low energy group there are multiplets formed by a spin-orbit splitting of ^{6}H and ^{6}F terms with the $^6H_{5/2}$ ground state. The high energy group encompasses very closely spaced multiplets derived from the ^{4}F, ^{4}G, ^{4}H, ^{4}I, ^{4}K, ^{4}L, ^{4}K, ^{4}M quartet and ^{6}P sextet terms with the lowest $^4G_{5/2}$ metastable state. Transition between quartet and sextet terms are spin forbidden therefore intensities of absorption and emission lines related to transitions bridging multiplets belonging to different groups are weak, except for the $^6H_{5/2}$ – $^6P_{3/2,\ 5/2}$ absorption line near 405 nm.

Figure 2 compares survey room temperature absorption spectra recorded in the UV-visible region for $(Lu_xGd_{1-x})_2SiO_5:Sm^{3+}$ crystals with x = 0.11 and x = 0.19. The spectra differ in the overall band intensity and in the band shape. In particular, the spectra of LGSO:Sm system with the LSO-type structure (x = 0.19) exhibit poorer line-structure than those of LGSO:Sm^{3+} with the GSO-type structure (x = 0.11). Nevertheless, peak values of absorption cross section for the $^6H_{5/2}$ – $^6P_{3/2,\ 5/2}$ transition around 405 nm for the two systems are high enough to assure efficient excitation of visible emission originating in the $^4G_{5/2}$ level.

#205162 - $15.00 USD Received 21 Jan 2014; revised 6 Mar 2014; accepted 6 Mar 2014; published 18 Mar 2014

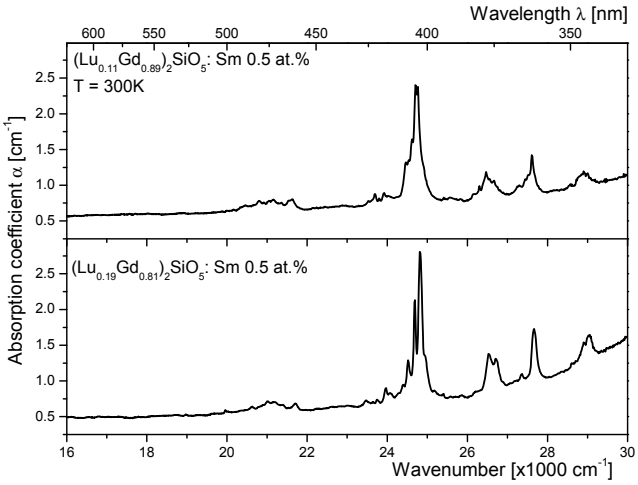

Fig. 2. Comparison of survey absorption spectra recorded in the UV-visible region for $(Lu_xGd_{1-x})_2SiO_5:Sm^{3+}$ crystals with x = 0.11 and x = 0.19

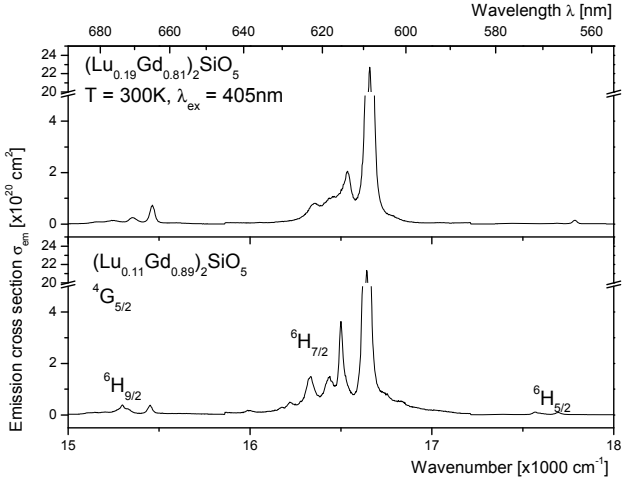

Fig. 3. Comparison of emission cross sections recorded for $(Lu_xGd_{1-x})_2SiO_5:Sm^{3+}$ crystals with x = 0.11 and x = 0.19. Values of emission cross section was obtained using Fuchtbauer– Ladenburg equation. For calculation experimental values of branching ratios was taken.

Figure 3. compares survey room temperature emission spectra recorded for crystals $(Lu_xGd_{1-x})_2SiO_5:Sm^{3+}$ with x = 0.11 and x = 0.19. The spectra consist of bands related to the $^4G_{5/2} \rightarrow {}^6H_{5/2}$ (~570 nm), $^6H_{7/2}$ (~600 nm) and $^6H_{9/2}$ (~650 nm) transitions of Sm^{3+} ions. Again, bands for the LGSO:Sm^{3+} with the GSO-type structure (x = 0.11) show much more complex structure of band components. In the following we will consider origins of this phenomenon.

3.2 Low temperature emission spectra

Figure 4 compares high-resolution emission spectra of $(Lu_xGd_{1-x})_2SiO_5$: 0.5at.% Sm^{3+} (x = 0.11 and 0.19) at 5 K, normalized to the strongest line at 600 nm. Samarium ions were

#205162 - $15.00 USD Received 21 Jan 2014; revised 6 Mar 2014; accepted 6 Mar 2014; published 18 Mar 2014

directly excited at 405 nm, a wavelength corresponding to the most intense absorption line in the UV-blue region. Its was found that its absorption coefficient at 405 nm amounts to 2.7 cm^{-1} when x = 0.11 (81% of Gd^{3+}) and to 4.2 cm^{-1} when x = 0.19 (89% of Gd^{3+}). A narrow and intense line

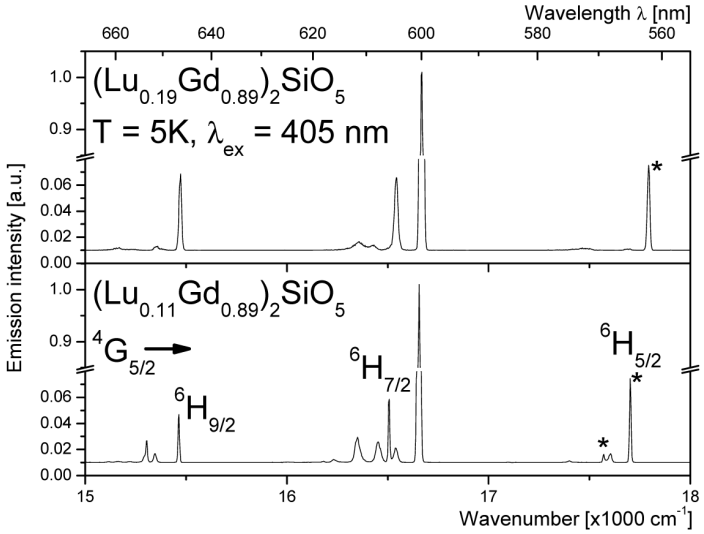

Fig. 4. High-resolution emission spectra of $(Lu_xGd_{1-x})_2SiO_5:Sm^{3+}$ crystals with different content of Gd^{3+} ions. Spectra were obtained at 5 K under the direct excitation of Sm^{3+} ions with 405 nm wavelength and normalized to the strongest line at about 600 nm. The asterisks indicate the 0-0 lines of the $^4G_{5/2} \rightarrow {}^6H_{5/2}$ transition.

at around 600 nm dominates the spectra however spectral positions, intensities and numbers of remaining lines are not the same. To account for experimental data we recall information regarding local surrounding of rare earth ions for the C2/c and $P2_1/c$ symmetries encountered in LGSO host. The nearest environment of Lu^{3+} ions in the LSO structure and Gd^{3+} ions in GSO structure are presented in Fig. 5.

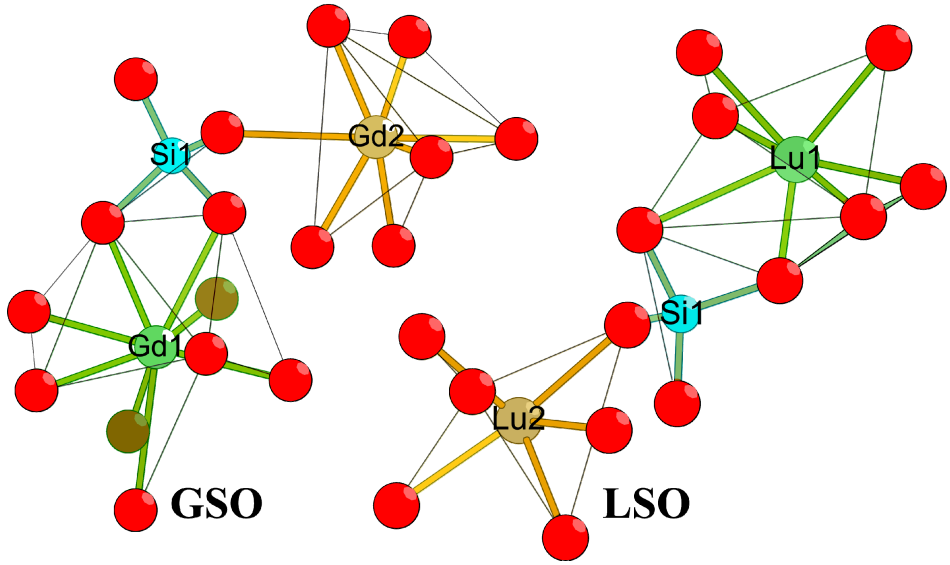

Fig. 5. Polyhedrons of Lu1 and Lu2 in Lu_2SiO_5 structure (right picture) and of Gd1 and Gd2 in Gd_2SiO_5 structure (left picture). Interatomic distances are in angstrom (Å).

#205162 - $15.00 USD Received 21 Jan 2014; revised 6 Mar 2014; accepted 6 Mar 2014; published 18 Mar 2014

In both structures there are two kind of oxygen ions: O1 - O4 connected with Si^{4+} and non-silicon bonded oxygen O5. The Lu_2SiO_5 crystal structure contains eight formula units (C2/c space group, Z = 8, 64 atoms including 16 atoms of Lu^{3+}) in monoclinic unit cell and is created by (SiO_4) and (OLu_4) tetrahedra. The (OLu_4) tetrahedra form chains running along c axis and interconnected by isolated (SiO_4) tetrahedra what makes the structure more rigid than that of GSO [17]. Two crystallographically different lutetium ions have oxygen coordination number CN of 7 (Lu1, LuO_7 polyhedra, average Lu-O distance of 2.32 Å) and of 6 (Lu2, LuO_6 polyhedra, average Lu-O distance of 2.23 Å) and both are located in lattice positions with the C1 point symmetry. The monoclinic unit cell of Gd_2SiO_5 ($P2_1/c$ space group, Z = 4) is two times smaller than that of LSO and contains 32 atoms including 8 atoms of Gd^{3+}. In this structure the (OGd_4) tetrahedra do not form chains but a two-dimensional network parallel to the (100) plane into which the (SiO_4) tetrahedra are packed [17]. The crystal cleavage along the (100) plane is a consequence of relatively weak bonding between layers. Gd^{3+} ions occupy both (GdO_9) nine-vertex coordination polyhedra (Gd1, average Gd-O distance of 2.49 Å) and (GdO_7) seven-vertex coordination polyhedra (Gd2, average Gd-O distance of 2.39 Å) in which Gd^{3+} ions residue in sites with C1 local symmetry. A quantitative studies of dopant distribution between available polyhedra are extremely rare and limited only to LSO and LGSO crystals in which large Ce^{3+} ions (1.01 Å) substitute small Lu^{3+} ions (0.86 Å) in their lattice positions. It has been found that Ce^{3+} ions (0.25 at%) in Lu_2SiO_5 crystal occupy both Lu1 and Lu2 sites with the Ce^{3+} distribution as 95% to LuO_7 polyhedra (Ce1) and 5% to LuO_6 (Ce2) polyhedra [18] or 80% to Ce1 and 20% to Ce2 sites [19]. It was demonstrated by Sidletskiy et. al [13,14] that in Ce:$(Lu_xGd_{1-x})_2SiO_5$ with different degree of cation substitution, Lu^{3+} ions favour the LnO_6 sixfold polyhedra whereas Gd^{3+} ions preferably occupy LnO_7 sevenfold ones as long as the C2/c lattice symmetry is protected. However, when the symmetry of LGSO changes to $P2_1/c$, the Lu^{3+} ions occupy sites coordinated by seven oxygens (LnO_7) whereas the Gd^{3+} are located in sites with nine-oxygen coordination. In accordance with [13,14], Gd^{3+} ions in the LGSO structure must tend to replace Lu^{3+} ions in Lu1 sites where the average Lu-O distance of 2.32 Å is larger than that of 2.23 Å for Lu2 site.

The $^4G_{5/2} \rightarrow {}^6H_{5/2}$ emission spectrum in LGSO containing 81 at% of Gd^{3+} is dominated by a strong and narrow line at 17794 cm^{-1} (562 nm). We assign this line to the transition between the lowest Stark's components of the initial and terminal level (0-0 line, denoted by asterisks in Fig. 4). Very weak emission that originates in the second samarium site contributes to this spectrum because a number of experimentally observed lines is larger than that expected for one site (four instead of three) but its identification is impossible. However, when the gadolinium content in the LGSO lattice reaches 89 at% or more, the luminescence from two non-equivalent Sm^{3+} sites is clearly seen in spectra; the number of lines is close to that predicted for two sites. Moreover, a careful examination of the $^6H_{5/2} \leftrightarrow {}^4G_{5/2}$ absorption and emission spectra at 5 K made it possible to identify unambiguously the lines at 17706 cm^{-1} (565 nm) and 17572 cm^{-1} (569 nm) as 0-0 transitions of Sm^{3+} ions residing in two sites in the GSO host [8] and in LGSO having the GSO-type symmetry. These findings are corroborated by changes in Gd^{3+} absorption spectra of the $^8S_{7/2} \rightarrow {}^6P_{3/2}$, $^6P_{5/2}$ and $^6P_{7/2}$ transitions at 5 K, presented in Fig. 6. The impact of the increasing Gd^{3+} content manifests in the change of number of optical lines, their energetic positions and their mutual intensity relationship. Ionic radii of Gd^{3+} (0.94 Å) and Sm^{3+} (0.96 Å) are similar. Therefore, one can expect that both Gd^{3+} and Sm^{3+} ions will tend to occupy the same site polyhedra in the LGSO matrix.

#205162 - $15.00 USD Received 21 Jan 2014; revised 6 Mar 2014; accepted 6 Mar 2014; published 18 Mar 2014

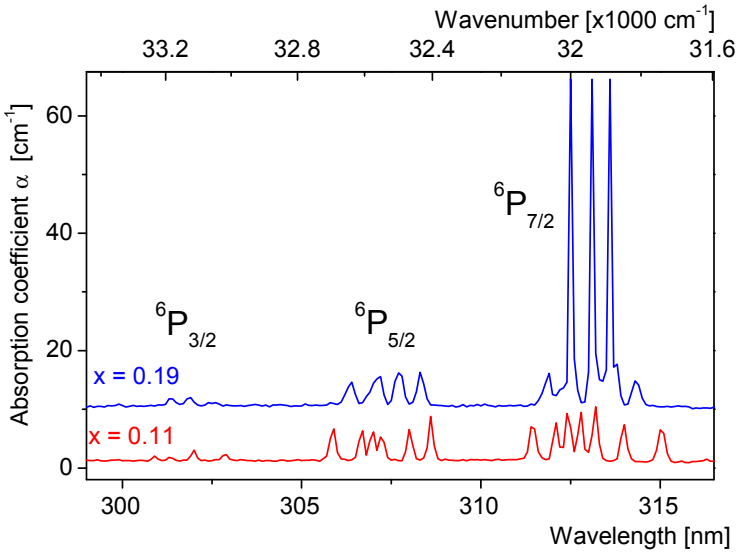

Fig. 6. Optical lines of the $^8S_{7/2} \rightarrow {}^6P_J$ absorption bands of Gd^{3+} ions in LGSO lattice with the C2/c (x = 0.19) and $P2_1/c$ structures (x = 0.11). T = 5 K.

Results presented above corroborate the diversity of distribution of rare earth ions in multi-fold polyhedra of LGSO lattice. However, a kinetics study of the Sm^{3+} emission in the 5 – 300 K temperature range indicates that the symmetry difference associated with non-equivalent Sm^{3+} sites in LGSO lattices affects weakly rates of transitions originating in the $^4G_{5/2}$ metastable state. In fact, luminescence decay curves recorded for the two systems follow a single exponential time-dependence with lifetime values ranging from about 1.91 ms at 5 K to about 1.80 ms at 300 K. It may be interesting to notice that room temperature radiative and experimental lifetimes of 1.78 ms and 1.74 ms, respectively were reported for Gd_2SiO_5:Sm crystal [8].

3.3. VUV excitation spectra and VUV –excited emission spectra

Figure 7 compares excitation spectra of the LGSO:Sm systems studied monitoring the 610 nm emission ($^4G_{5/2} \rightarrow {}^6H_{7/2}$) from Sm^{3+} ions. Broad bands with maxima at around 200 nm were attributed to the transfer of electron from the valence band VB of the LGSO host to trivalent Sm ion (CT transition). In consequence, a Sm^{2+} ions is created and the energy of the CT transition approximately gives the energy gap between the top of VB and the $4f^6$ ground state of Sm^{2+} ion. The data obtained at 12 K lead to the value of 6.11 eV for $(Lu_xGd_{1-x})_2SiO_5$:Sm that is somewhat lower than 6.95 eV reported for $Lu_2Si_2O_7$ [18] and 7.35 eV reported for $LiYP_4O_{12}$ [19] but close to 5.59 eV and 6.2 eV determined for $CaSO_4$ and $Ln_2(SO_4)_3$ and collected by Dorenbos in [20]. It is worth to mention that optical bandgaps for both crystals are similar and equal ~6.1 eV (210 nm) [4, 21]. Structural transformation of LGSO from the LSO-type to GSO-type structure affects short-wavelength side of LGSO:Sm spectra. Wide-ranging CT band of $(Lu_{0.19}Gd_{0.81})_2SiO_5:Sm^{3+}$ includes a sub-structure at around 9,6 eV that turns into well-defined CT band and high-energetic structure of lattice when the content of Gd^{3+} ions increases to 89%, corroborating changes in the host ordering.

#205162 - $15.00 USD Received 21 Jan 2014; revised 6 Mar 2014; accepted 6 Mar 2014; published 18 Mar 2014

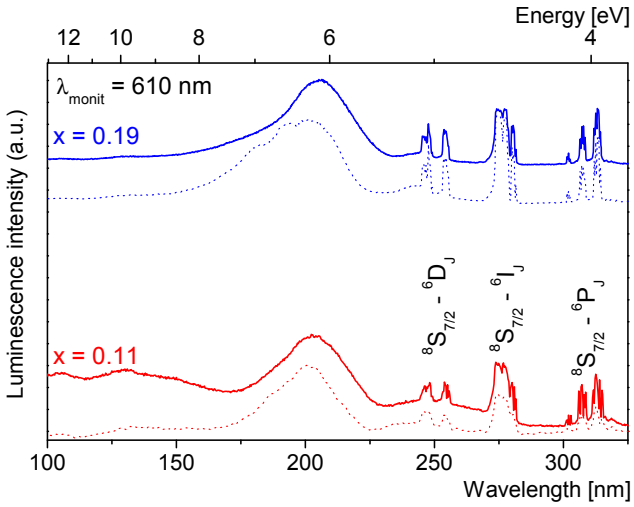

Fig. 7. Excitation spectra of $(Lu_xGd_{1-x})_2SiO_5:Sm^{3+}$ crystals with x = 0.11 and x = 0.19 excited by synchrotron radiation at 12 K (dotted lines) and 300 K (solid lines) registered under monitoring samarium luminescence at 610 nm.

The $4f^5 \rightarrow 4f^4 5d^1$ transitions of Sm^{3+} do not clearly become apparent in the VUV excitation spectra of LGSO:Sm. Even though systematic studies on the 5d samarium states are quite scarce and limited only to a few fluoride compounds, the position of the allowed 5d state in LGSO:Sm may be estimated based on the knowledge of the $^2F_{5/2} \rightarrow$5d absorption energy in Ce^{3+} -doped LSO and GSO [1]. Taking into account that the first $4f^5 \rightarrow 4f^4 5d^1$ transition of Sm^{3+} is predicted to have ca 3.22 eV higher energy than that of Ce^{3+} [20], the energy of the lowest 5d samarium state in LSO and GSO were estimated, to find a correlation between synchrotron excitation spectra (12 K) and a potential energetic position of 5d state in studied Sm:LGSO systems. The results are presented in Tab. 1. Connecting multi-site structure of LGSO (two Lu^{3+} and two Gd^{3+} sites in LSO and GSO, respectively) with the sensitivity of $4f^n \rightarrow 4f^{n-1}5d^1$ to local environment, we assigned an optical structure in the 6.28 – 6.78 eV range to the interconfigurational excitation to the first and second component of the 5d state.

There is no doubt that sharp and well-defined lines at around 250, 275 and 310 nm correspond to Gd^{3+} transitions within $4f^7$ ground electronic configuration, in particular to the $^8S_{7/2} \rightarrow {}^6P_J$, ^6I_J, ^6D_J transitions. Their presence in the excitation spectra of Sm^{3+} emission at 610 nm points out an efficient energy transfer from Gd^{3+} to Sm^{3+} ions.

Table 1. Spectral position and energy of the lowest 5d-state of Ce^{3+} and Sm^{3+} in Lu_2SiO_5 (LSO) and Gd_2SiO_5 (GSO) and $(Lu_xGd_{1-x})_2SiO_5$ (LGSO) hosts.

Host	Ion (Site)	Spectral position (nm)	Energy (eV)	Data status
LSO	Ce(1) Ce(2)	356 (λ_{abs}) 376 (λ_{abs})	3.48 3.30	ref [1].
GSO	Ce(1) Ce(2)	345 (λ_{abs}) 384 (λ_{abs})	3.59 3.23	ref [1].
LSO	Sm(1) Sm(2)	185 198	6.70 6.25	This work, estimated values
GSO	Sm(1) Sm(2)	182 192	6.81 6.45	This work, estimated values
LGSO	Sm(1)&Sm(2)	198 - 182	6.25 – 6.81	This work (excitation spectra at 12 K)

#205162 - $15.00 USD Received 21 Jan 2014; revised 6 Mar 2014; accepted 6 Mar 2014; published 18 Mar 2014

Comparable intensities of the CT and $^6I_J \rightarrow {}^8S_{7/2}$ transitions in the VUV-UV excitation spectra of Sm^{3+} emission imply that an energy transfer from these bands should bring forth an efficient long-wavelength luminescence. Figure 8 shows luminescence spectra of LGSO:Sm containing 81 and 89 at% of Gd^{3+} acquired at 12 K under the synchrotron radiation excitation and related to the $^4G_{5/2} \rightarrow {}^6H_{5/2}$ (~570 nm), $^6H_{7/2}$ (~600 nm), $^6H_{9/2}$ (~650 nm), and $^6H_{11/2}$ (~706 nm). The spectra are representative for excitations in the 40-110 nm (host), 170-200 nm (4*f*5*d*, CT bands) and 240-313 nm (Gd^{3+} lines) ranges on the one hand, and for the crystals with the same type-structure on the other. Although the CCD camera employed gives a slight instrumental broadening it can be seen easily that the spectra of LGSO:Sm^{3+} with the LSO-type structure exhibit poorer line-structure than those of LGSO:Sm^{3+} with the GSO-type structure. The excitation wavelength has no effect on the line positions and intensities within the LSO-type host. Small differences between emission spectra of $(Lu_{0.11}Gd_{0.89})_2SiO_5$: Sm sample, taken under 112 – 196 and 277-312 [nm] excitations, could be found however. Excitation in 112 – 196 nm is conneted with broad and intense bands realted to intervalence and CT transitions. Excitation in 277 and 312 nm is related with energy transfer from Gd^{3+} to Sm^{3+}. From observed differences emerge, that gadolinium ions preferentially transfer energy to samarium ion occupying one site, when energy transfer to Sm^{3+} located in second site is scarce.

Results presented and discussed in this section justify conclusions regarding possible impact of an adverse phenomenon of excited state absorption on emission efficiency in LGSO:Sm^{3+} optically pumped at wavelengths above 400 nm. Unsuccessful attempts to achieve the optical amplification of visible emission in praseodymium-doped GSO and YSO hosts, reported in the past, have been attributed to strong ESA transitions from the metastable $^3P_0$ level to $4f^15d^1$ states of Pr^{3+} [3]. In this phenomenon the most relevant channels are ESA of pump radiation and ESA at wavelengths of emitted light. For a pump radiation at 405 nm the ESA from the $^4G_{5/2}$ metastable level of Sm^{3+} located near 17700 cm^{-1} in LGSO is able to feed states having energies ca 42340 cm^{-1}. It can be seen in Fig. 7 that this value is lower than the onset of the CT band for the systems under study. For an emitted light around 600 nm the ESA is able to feed excited Sm^{3+} states having energies ca 34300 cm^{-1}. Intensities of transitions within the $4f^5$ configuration of Sm^{3+} are predicted to be markedly smaller than those of CT or 4*f*-5*d* transitions, however. Accordingly, we suppose that in contrast to Pr^{3+} ions the ESA in samarium doped LGSO host is not crucial.

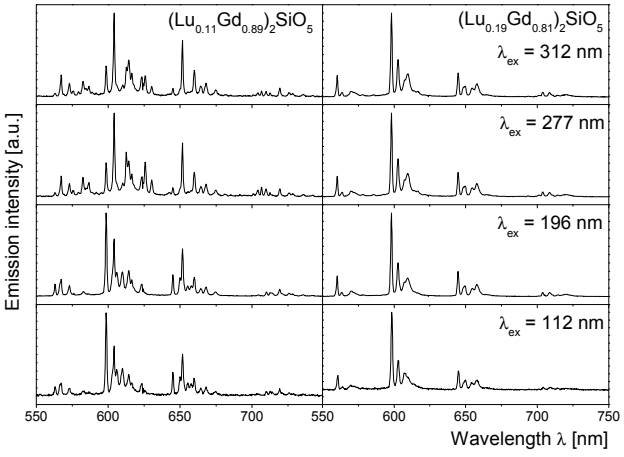

Fig. 8. Emission spectra of Sm^{3+} in the LGSO crystals having the LSO- and GSO-type symmetry (x = 0.19 and 0.11, respectively) registered at 12 K under different wavelengths of synchrotron radiation.

#205162 - $15.00 USD Received 21 Jan 2014; revised 6 Mar 2014; accepted 6 Mar 2014; published 18 Mar 2014

3.4. Optical amplification

Optical amplification experiments were performed to verify the supposition forwarded in previous section. The emission spectra obtained in the Sm^{3+} doped crystals have several emission bands in the visible region as can be seen in Fig. 3 These spectra have been obtained in the sample conditions (for comparison purposes) and all the bands can be clearly identified with transitions from the $^4G_{5/2}$ level of Sm^{3+} ions.

In the emission spectra shown in Fig. 3 it is interesting to note the intense emissions about 600 nm obtained in the two doped crystals. This emission band corresponding to the $^4G_{5/2} \rightarrow {}^6H_{7/2}$ transition could be interesting for optical applications because exciting to upper levels to the $^4G_{5/2}$ level could be possible to obtain a laser system of four levels with an emission about 600 nm.

As was explained in the experimental section, an experiment setup of pump and probe has been made in order to characterize the possible optical amplification abput 600 nm in these crystals. The optical gain, using a stimulation probe about 600 nm, can be obtained evaluating the signal enhancement (SE) when the probe beam passes through the crystal. Therefore, it is defined by [16, 22]:

$$SE = \frac{I_{pp} - I_p}{I_{probe}} \tag{1}$$

where I_{pp} is the intensity detected about 600 nm in the direction of the probe beam coming out from the sample when it is irradiated simultaneously with the pump (about 473 nm) and the probe (about 600 nm) beams, I_p is the spontaneous emission intensity at the same wavelength when the probe is blocked before the sample, and I_{probe} is the intensity of the probe beam. The intensity of the probe beam through a material decreases according to the exponential law:

$$I_{probe} = I_0 e^{-\alpha L} \tag{2}$$

where I_0 is the probe intensity in the entrance of the crystal, α is the absorption coefficient at this wavelength and L is its length.

When the crystal is affected by both pump and the probe beams then I_{pp} can be expressed in the following form:

$$I_{pp} = I_p + I_0 e^{(g-\alpha)L} \tag{3}$$

Where g is the gain due to the stimulated emission of the sample at the probe wavelength. At 600 nm the crystals are highly transparent and the value for α is negligible (see absorption spectra shown Fig. 9). Therefore, by introducing the Eqs. (2) and (3) into (1), the following expression for the gain is obtained:

$$SE = e^{gL} \tag{4}$$

#205162 - $15.00 USD Received 21 Jan 2014; revised 6 Mar 2014; accepted 6 Mar 2014; published 18 Mar 2014

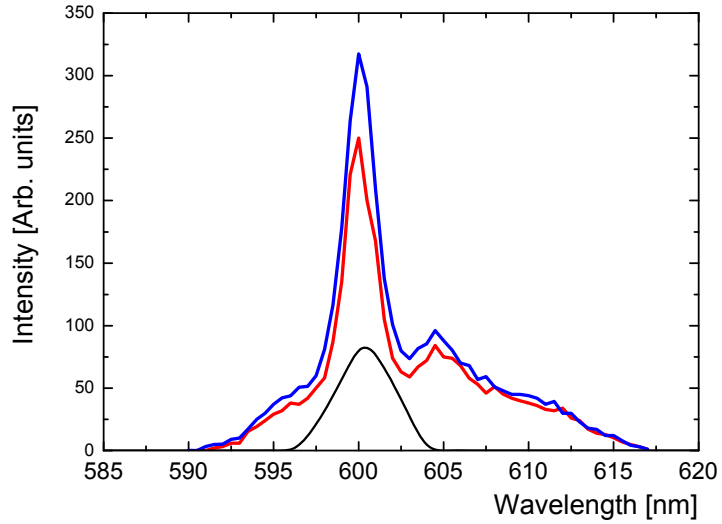

Fig. 9. Emission spectra of the $^4G_{5/2} - {}^6H_{7/2}$ transition of Sm^{3+} in $(Lu_xGd_{1-x})_2SiO_5$ (x = 0.19) crystal having the LSO-type of symmetry. The red line describes emission of the crystal under pump excitation (E_{pump}) at 473 nm. Black line is emission spectrum of probe (E_{probe}). The blue describes its emission under pump excitation at 473 nm and probe at 600 nm after substraction of black line ($E_{pump + probe} - E_{probe}$). The differecnce between blue and red spectra shows signal enchancement.

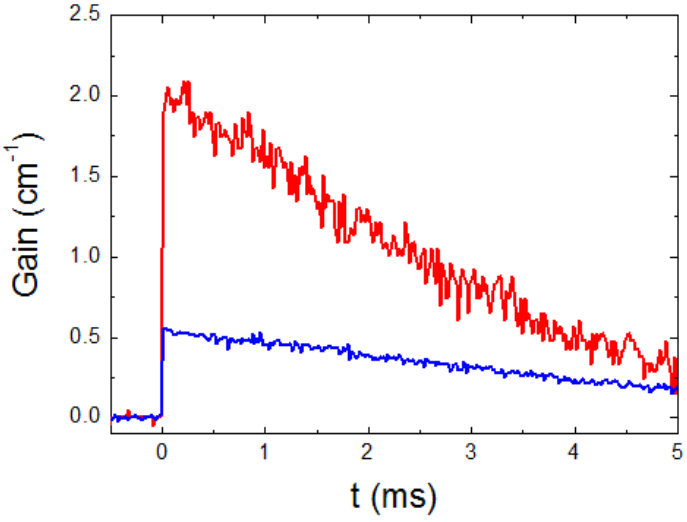

Fig. 10. Temporal dependence of the gain obtained for Sm^{3+} in $(Lu_xGd_{1-x})_2SiO_5$ (x = 0.19) after pulsed excitation at 473 nm and detecting at 596 nm. The red (dotted) curve was obtained with a pump energy density of 50 mJ/cm^2 and the blue (solid) curve with 20 mJ/cm^2

The values for I_{pp}, I_p and I_{probe} can be obtained as function of the time after pulsed excitation at 473 nm and detecting at 600 nm. In these experiments the probe has been tuned at 600 nm. Therefore, it is possible to obtain the optical gain as function of the time and using

#205162 - $15.00 USD Received 21 Jan 2014; revised 6 Mar 2014; accepted 6 Mar 2014; published 18 Mar 2014

the Eq. (4). The results are shown in Fig. 10 for two different pump intensities. As can be seen, immediately after the excitation pulse the optical gain is much higher due to there is a maximum in population of the excited level ($^4G_{5/2}$). When this level starts to depopulate the gain also decreases.

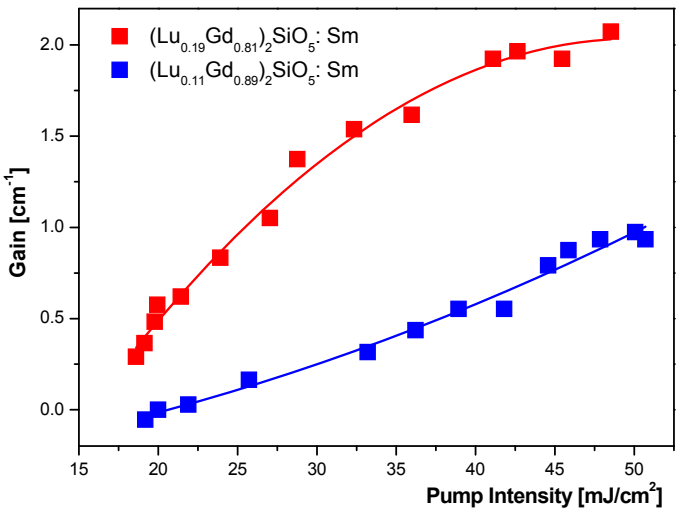

Fig. 11. Optical gain as a function of the pump energy density from 20 mJ/cm^2 to 50 mJ/cm^2 with a probe density of 150 μW/cm^2. The continuous lines are guide for the eye.

In Fig. 11 are shown the values obtained for the gain values at short times as function of the pump power density at 473 nm. As can be seen in the sample $(Lu_{0.19}Gd_{0.81})_2SiO_5$ are obtained better results respect to the $(Lu_{0.11}Gd_{0.89})_2SiO_5$ crystal. Both samples have similar lifetimes for the $^4G_{5/2}$ level (about 1.8 ms). But, as can be seen in Fig. 3, the intensity of the emission at 600 nm is higher for the $(Lu_{0.19}Gd_{0.81})_2SiO_5$ sample. This sharpness at 600 nm for the sample $(Lu_{0.19}Gd_{0.81})_2SiO_5$ respect to the $(Lu_{0.11}Gd_{0.89})_2SiO_5$ could explain the better results obtained of the optical gain at 600 nm in Fig. 11.

4. Conclusions

Single crystals of $(Lu_xGd_{1-x})_2SiO_5:Sm^{3+}$ (LGSO:Sm) with x = 0.11 and x = 0.19 and Sm^{3+} concentration of 0.5 at% were grown by the Czochralski technique at temperatures lower than that of the Lu_2SiO_5 host (below 1780 °C against 2050 °C). XRD examination revealed that the structure of the LGSO:Sm is consistent with the $P2_1/c$ space group for x = 0.11 and with the C2/c space group for x = 0.19. Based on low temperature emission spectra it was concluded that as the $(Lu_xGd_{1-x})_2SiO_5:Sm^{3+}$ crystal keeps the C2/c symmetry of LSO lattice, almost all emission intensity comes from samarium ions located in (LuO7) polyhedra. The determined energy of the $^4G_{5/2}(0) \rightarrow {}^4H_{5/2}(0)$ transition of Sm^{3+} in this site position is 17790 cm^{-1}. Intensity of emission coming from a second type of Sm^{3+} sites (LuO6 polyhedra) was extremely low. In LGSO:Sm crystals having the $P2_1/c$ space group two available Sm^{3+} sites contribute to emission. The low temperature lines at 17706 and 17572 cm^{-1} were attributed to $^4G_{5/2}(0) \rightarrow {}^6H_{5/2}(0)$ transitions of Sm^{3+} ions located in two non-equivalent sites. In spite of the fact that Sm^{3+} ions are located in non-equivalent lattice positions of two different structures of LGSO lattice, luminescence decays exhibit single exponential character with similar time constants implying that differences in local symmetry of Sm^{3+} ions weakly affect rates of transitions originating from the $^4G_{5/2}$ luminescence state.

#205162 - $15.00 USD Received 21 Jan 2014; revised 6 Mar 2014; accepted 6 Mar 2014; published 18 Mar 2014

Excitation spectra of Sm^{3+} emission recorded in the VUV-UV region between 100 nm and 350 nm made it possible to locate the energy of CT transition at about 6.11 eV and to assess the low energy limit for the $4f^5 \rightarrow 4f^4 5d^1$ transitions of Sm^{3+} to about 6.81 eV. It was concluded that in the two systems studied these energies are advantageously high thereby preventing the contribution of intense allowed transitions to an adverse excited state absorption of both blue pump radiation and yellow emission. Experiments of optical amplification of yellow emission, performed employing a pump-and-probe technique corroborated this conclusion. It was found that for a LGSO:Sm^{3+} crystal having the C2/c symmetry an increase of the pump power density from 20 mJ/cm^2 to 50 mJ/cm^2 at a constant power probe density of 150 μW/cm^2 brings about a positive gain growing from about 0.25 to 2 [cm^{-1}]. In the same conditions a maximum gain value of 1 cm^{-1} was measured for LGSO:Sm^{3+} crystal having the $P2_1/c$ symmetry. It was concluded that the former system is promising for the design of all-solid-state yellow lasers.

Acknowledgments:

The work is supported by National Science Centre of Poland (NCN) within a project Number DEC-2011/01/B/ST7/06166.

Authors thank Ministerio de Economia y Competitividad of Spain (MINECO) within The National Program of Materials (MAT2010-21270-C04-02/-03/-04), The Consolider Ingenio 2010 Program (MALTA CSD207-0045, www.malta-consolider.com) the EU-FEDER for their financial support and ACIISI of Gobierno de Canarias for the project ID20100152